Tuning the Microenvironment to Create Functionally Distinct Mesenchymal Stromal Cell Spheroids

VICTORIA L. THAI [iD],[1,2] DIEGO O. CANDELAS,[1] and J. KENT LEACH [iD][1,2]

[1]Department of Biomedical Engineering, University of California, Davis, Davis, CA 95616, USA; and [2]Department of Orthopaedic Surgery, UC Davis Health, 4860 Y Street, Suite 3800, Sacramento, CA 95817, USA

Associate Editor Michael S. Detamore oversaw the review of this article.

ABBREVIATIONS

ECFC	Endothelial colony forming cells
MSC	Mesenchymal stromal cells
$CoCl_2$	Cobalt(II) chloride
VEGF	Vascular endothelial growth factor
$VEGF_{MAX}$	Spheroids that maximize VEGF production
$VEGF_{MIN}$	Spheroids that minimize VEGF production
PGE_2	Prostaglandin E2
$PGE_{2,MAX}$	Spheroids that maximize PGE_2 production
$PGE_{2,MIN}$	Spheroids that minimize PGE_2 production
EGF	Epidermal growth factor
CD31 (PE-CAM-1)	Cluster of differentiation 31 (platelet endothelial cell adhesion molecule)
HGF	Hepatocyte growth factor
PEG-4MAL	4-arm poly(ethylene glycol) maleimide
MMP	Matrix metalloproteinase
DOE	Design of experiments

Abstract—Mesenchymal stromal cells (MSCs) are under investigation for wound healing and tissue regeneration due to their potent secretome. Compared to monodisperse cells, MSC spheroids exhibit increased cell survival and enhanced secretion of endogenous factors such as vascular endothelial growth factor (VEGF) and prostaglandin E2 (PGE_2), two key factors in wound repair. We previously upregulated the proangiogenic potential of homotypic MSC spheroids by manipulating microenvironmental culture conditions. However, this approach depends on the responsiveness of host endothelial cells (ECs)—a limitation when attempting to restore large tissue deficits and for patients with chronic wounds in which ECs are dysfunctional and unresponsive. To address this challenge, we used a Design of Experiments (DOE) approach to engineer functionally distinct MSC spheroids that maximize VEGF production ($VEGF_{MAX}$) or PGE_2 production ($PGE_{2,MAX}$) while incorporating ECs that could serve as the basic building blocks for vessel formation. $VEGF_{MAX}$ produced 22.7-fold more VEGF with enhanced endothelial cell migration compared to $PGE_{2,MAX}$, while $PGE_{2,MAX}$ produced 16.7-fold more PGE_2 with accelerated keratinocyte migration compared to $VEGF_{MAX}$. When encapsulated together in engineered protease-degradable hydrogels as a model of cell delivery, $VEGF_{MAX}$ and $PGE_{2,MAX}$ spheroids exhibited robust spreading into the biomaterial and enhanced metabolic activity. The distinct bioactivities of these MSC spheroids demonstrate the highly tunable nature of spheroids and provide a new approach to leverage the therapeutic potential of cell-based therapies.

Address correspondence to J. Kent Leach, Department of Orthopaedic Surgery, UC Davis Health, 4860 Y Street, Suite 3800, Sacramento, CA 95817, USA. Electronic mail: jkleach@ucdavis.edu

INTRODUCTION

Mesenchymal stromal cells (MSCs) are commonly used for wound healing applications due to their differentiation capability and therapeutic secretome that reduces inflammation, enhances angiogenesis, and promotes tissue formation.[18,35] Their versatile nature has been harnessed in numerous applications including myocardial infarction, bone regeneration, and cuta-

neous wound healing.[2,9,15] Furthermore, the addition of endothelial cells (ECs) to MSCs increases angiogenic and osteogenic regeneration in critically sized bone defects.[6,28,29] While monodispersed MSCs embody multifaceted roles in various therapeutic approaches, we and others have established the advantages of using MSCs as aggregates, also known as spheroids.[14]

Spheroids exhibit increased overall function due to improved cellular viability in harsh environments and enhanced secretion of endogenous growth factors (GFs).[12,16] Among other factors, MSC spheroids secrete more vascular endothelial growth factor (VEGF) and prostaglandin E2 (PGE_2), two important bioactive factors in wound healing.[37] VEGF stimulates angiogenesis, while PGE_2 mediates local inflammation and promotes the recruitment of cells that are critical for re-epithelialization.[23,30] We previously reported a combination of microenvironmental conditions to form MSC spheroids with enhanced secretion of both VEGF and PGE_2 for cutaneous wound healing.[25] Spheroid size, oxygen tension, and inflammatory cues influence the MSC spheroid secretome. However, because our previous spheroid formulation was designed to simultaneously upregulate VEGF and PGE_2 secretion, it does not fully capitalize on the therapeutic capabilities of MSCs. By developing individual spheroids, we can more precisely tune the conditions to maximize the secretion of a preferred growth factor for therapeutic use. These spheroids could be used in a modular approach to achieve the desired cytokine concentration. Furthermore, our previous approach is limited by its dependence on the responsiveness of host ECs for neovascularization. Individuals susceptible to chronic, nonhealing wounds are often diagnosed with diabetes, cardiovascular diseases, renal disease, or are obese. These debilitating diseases give rise to EC dysfunction, which causes native ECs to become unresponsive to potent bioactive factors secreted by spheroids and consequently hinders angiogenesis.[10] The challenges presented by chronic wounds motivate the need for a therapy that promotes vascularization and epithelialization without depending on host ECs.

When co-cultured with endothelial colony forming cells (ECFCs), MSCs promote neovascularization, yielding stable vascular structures.[17,20,33,36] However, this approach fails to fully address the critical need for epithelialization due to rapid cell death when transplanted in harsh microenvironments. To address this challenge, we engineered MSC spheroids with distinct secretomes and incorporated ECFCs to provide the basic building blocks for neovascularization. We hypothesized that MSC spheroids engineered with different therapeutic potentials (*i.e.*, maximizing VEGF or PGE_2 secretion) containing ECFCs would promote vascularization and epithelialization. Herein, we used a Design of Experiments (DOE) multivariable analysis to engineer these

unique spheroids and determine the interaction between multiple input variables shown to influence the MSC secretome. Following optimization, the functionally distinct spheroids were then entrapped in MMP-degradable poly(ethylene glycol) (PEG) hydrogels to explore spheroid interactions with their microenvironment. This study offers the unique opportunity to independently tune MSC spheroids and leverage them in a modular fashion to maximize specific growth factor secretion for regenerative therapies.

MATERIALS AND METHODS

Cell Culture

Human endothelial colony forming cells (ECFCs) were isolated from human cord blood obtained through the UC Davis Cord Blood Collection Program (UCBCP).[24] Cells were expanded in EGM-2 supplemented media (Promo-Cell, Heidelberg, Germany) with gentamicin (50 μg/mL; ThermoFisher, Waltham, MA) and amphotericin B (50 ng/mL; ThermoFisher) under standard culture conditions (37 °C, 5% CO_2, 21% O_2) until use at passages 7–8. Media changes were performed every 2 days. Human bone marrow-derived MSCs from two male donors (21-year-old, RoosterBio, Inc., Frederick, MD and 22-year-old, Texas A&M University, College Station, TX) were expanded without further characterization in standard culture conditions in minimum essential alpha medium (α-MEM; Invitrogen, Carlsbad, CA) supplemented with 10% fetal bovine serum (FBS; Atlanta Biologicals, Flowery Branch, GA) and 1% penicillin/streptomycin (P/S; Gemini Bio-Products, Sacramento, CA) until use at passages 4–5. Media changes were performed every 2–3 days. Diabetic human dermal microvascular cells (HMVECs) (Lonza, Walkersville, MD) from a single donor (66-year-old female) were expanded without further characterization in standard culture conditions in EGM-MV2 supplemented media (PromoCell) with gentamicin (50 μg/mL) and amphotericin B (50 ng/mL). Media changes were performed every 2 days. HaCaT cells (AddexBio Technologies, San Diego, CA), an immortalized human keratinocyte line from a single donor (62-year-old male), were expanded without further characterization in standard culture conditions in Dulbecco's Modified Eagle Medium (DMEM; Invitrogen) supplemented with 10% FBS and 1% P/S. HaCaTs were used at passages 15–18. Media changes were performed every 2–3 days. Aliquots were derived from the same batch of serum to ensure consistency.

Design of Experiments (DOE) Model

We used a Box-Behnken experimental design created with Design-Expert software version 11 (Stat-

Ease, Minneapolis, MN) to analyze the contribution of three variables (cell number, percentage of ECFCs, and cobalt(II) chloride (CoCl$_2$) concentration) on the secretion of VEGF from spheroids (Fig. 1a). These three input variables were chosen due to their ability to modulate the secretome of MSC spheroids. Cell number ranged from 1,000 to 15,000 cells based on enhanced sprouting and sprout length and restored vasculogenic potential of EC-MSC spheroids.[31,34] The percentage of ECFCs was varied from 0 to 100% where 0% represents spheroids with MSCs alone and 100% represents spheroids with ECs alone. CoCl$_2$ (0– 100 μM), a hypoxia-mimetic agent, was selected to stabilize HIF-1α and promote the production of pro-angiogenic cytokines.[38] The significance and interaction of the three input variables on VEGF secretion was assessed with response surface plots generated by the Design-Expert software. PGE$_2$ spheroid formulations were designed based on a DOE outlined in our previous work along with the addition of ECFCs. We modeled the effects of cell number and Pam3-Cys-Ser-Lys4 (Pam3CSK4; InvivoGen, San Diego, CA), a bacterial mimetic Toll-like receptor 2 (TLR2) antagonist, on PGE$_2$ production.[25] VEGF and PGE$_2$ secretion were measured using cytokine-specific enzyme-linked immunoassay (ELISA) kits according to the manufacturer's protocol (R&D Systems, Minneapolis, MN).

Validation of DOE Model and Characterization of Spheroid Secretome

Spheroids were formed from conditions predicted to maximize and minimize secretion of VEGF or PGE$_2$ as detailed in Tables 1 and 2, respectively. Culture media was refreshed 24 h prior to collection, and VEGF and PGE$_2$ concentrations in conditioned media (CM) were measured by ELISA. The secretory profile of each distinct spheroid was further characterized with a ProcartaPlex$^{\mathrm{TM}}$ human angiogenesis panel 18-plex kit to measure angiopoietin-1, BMP-9, EMMPRIN, follistatin, HB-EGF, LYVE-1, TIE-2, CD31, EGF, FGF-2, G-CSF, HGF, IL-8, leptin, PDGF-BB, syndecan, VEGF-A, and VEGF-D (CN: EPX180-15806-901; ThermoFisher) and assessed on the Luminex® xMAP 200 (ThermoFisher). The net mean fluorescence intensity (MFI) was measured and calculated for the 7 standards and samples, and the data were analyzed using the online ProcartaPlex$^{\mathrm{TM}}$ Analysis Application.

Spheroid Formation

Combinations of cell number, percentage of ECFCs, and CoCl$_2$ concentration were varied to form spheroids that maximized (VEGF$_{MAX}$ and PGE$_{2,MAX}$)

and minimized (VEGF$_{MIN}$ and PGE$_{2,MIN}$) VEGF and PGE$_2$ secretion using a DOE approach and our previous work.[25] VEGF$_{MAX}$, VEGF$_{MIN}$, PGE$_{2,MAX}$, and PGE$_{2,MIN}$ spheroid formulations are described in Tables 1 and 2. Spheroids were formed using a forced aggregation method.[32] Briefly, respective numbers of ECFCs and MSCs were pipetted into 1.5% agarose molds in well plates, and the plates were centrifuged at 500xg for 8 min. Plates were maintained in static culture conditions (37 °C, 5% CO$_2$, 21% O$_2$) for 48 h for spheroid formation in 3:1 EGM-2:α-MEM (3:1 media). Spheroids were then stimulated with either CoCl$_2$ or Pam3CSK4 for 72 or 48 h, respectively (Fig. 1b). Media from spheroids was refreshed (1 mL) 24 h prior to collection as CM.

Characterization of Spheroid Diameter, Cell Distribution, and Mechanical Properties

Prior to spheroid formation, ECFCs were stained with CellTrace$^{\mathrm{TM}}$ Violet and MSCs with CellTrace$^{\mathrm{TM}}$ Far Red (both from Invitrogen). After two days of spheroid formation, images of the spheroids were acquired via bright-field microscopy (Nikon Eclipse TE2000U). Images were processed and analyzed to quantify spheroid diameter in ImageJ (NIH, Bethesda, MD). Spheroid diameters were determined from analysis of images captured in the xy-plane at the largest cross-sectional area. Confocal images were also taken of the spheroids to visualize the composition of cells in the spheroids (Leica STELLARIS, Leica Camera AG, Wetzlar, Germany). Mechanical characterization of the spheroids was performed using a MicroTester (CellScale, Waterloo, Canada).[13]

VEGF Bioactivity Validation via Scratch Migration and Transwell Migration Assays

We determined the bioactivity of VEGF secreted by MSC spheroids via cell migration assays using ECFCs and diabetic HMVECs. ECFCs were seeded in 24-well plates at 5×10^4 cells/well, and diabetic HMVECs were seeded in 48-well plates at 1.5×10^4 cells/well. Cells were allowed to reach confluency and treated with mitomycin C (5 μg/mL), a cell proliferation inhibitor agent, for 30 min. Mitomycin C was replaced with fresh culture medium, and the confluent monolayer was uniformly scraped with a 200 μL pipette tip. Following wounding, wells were washed with culture medium to remove cell debris, and media was replaced with the respective treatment conditions. Fully supplemented media and 5 ng/mL recombinant VEGF (rVEGF) were used as positive controls while non-supplemented EGM-2 (EGM-2$_{non-supp}$) or EGM-MV2 (EGM-MV2$_{non-supp}$) were used as negative controls for
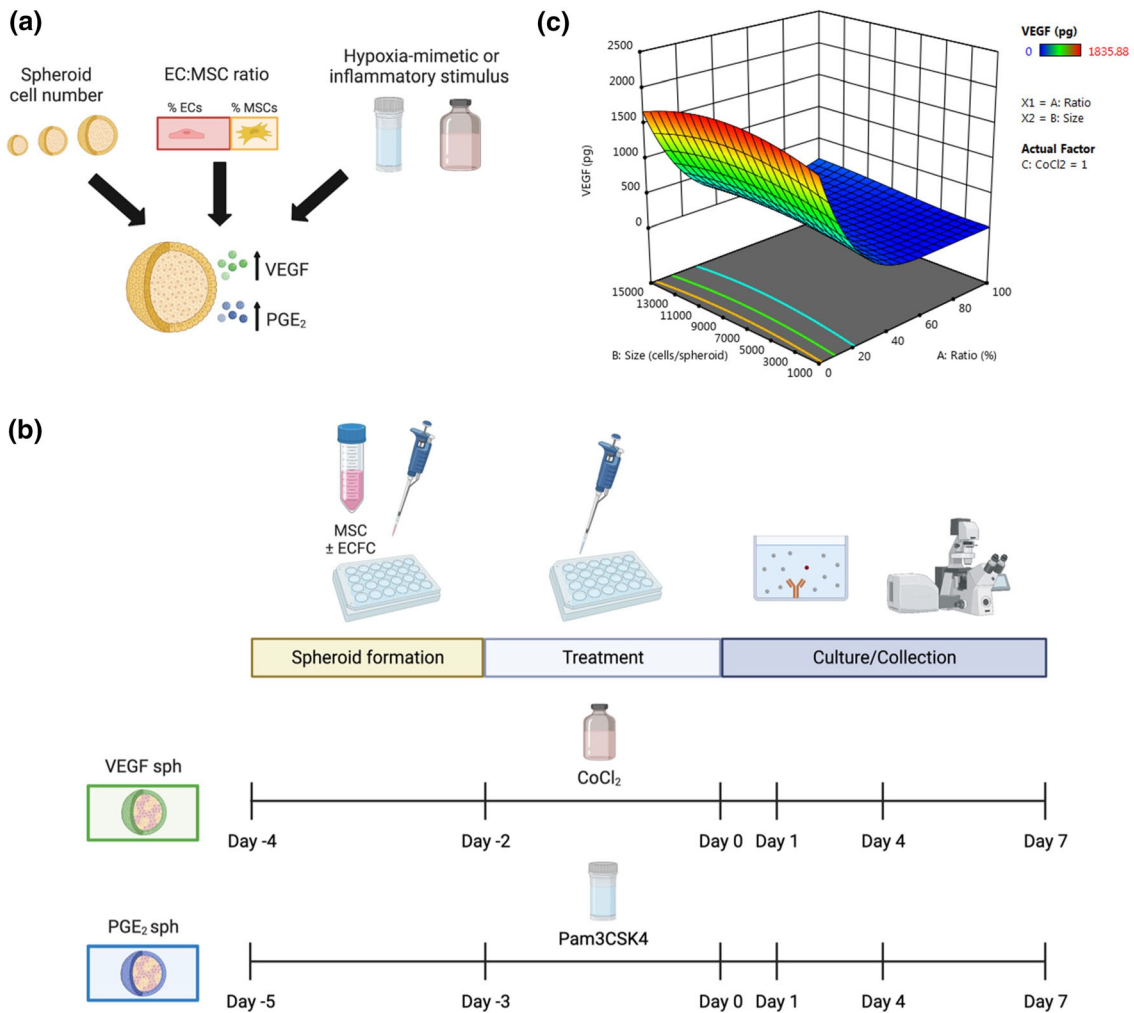
FIGURE 1. Design and fabrication of distinct MSC spheroids using a DOE approach. (a) Microenvironmental conditions were tuned to develop unique MSC spheroids. (b) Experimental outline of spheroid formulation. (c) 3D response surface map of microenvironmental condition effects on total VEGF secretion from MSC spheroids using 100 μM CoCl$_2$.

TABLE 1. Formulations for optimizing VEGF secretion from ECFC-MSC spheroids.

Group	# Cells/spheroid	% ECFCs	CoCl$_2$ concentration (μM)
VEGF$_{MAX}$	8,000	0	95.4
VEGF$_{MIN}$	2,850	66	8.8

TABLE 2. Formulations for optimizing PGE$_2$ secretion from ECFC-MSC spheroids.

Group	# Cells/spheroid	% ECFCs	Pam3CSK4 concentration (μg/mL)
PGE$_{2,MAX}$	60,000	33	1
PGE$_{2,MIN}$	15,000	33	0

ECFCs or diabetic HMVECs, respectively. Experimental groups consisted of 3:1 1% FBS-containing EGM-2$_{non-supp}$ or EGM-MV2$_{non-supp}$:treatment where treatment was 100:0, 50:50 (or 1:1), or 0:100 VEGF$_{MAX}$:PGE$_{2,MAX}$ CM. A minimum of three regions per scratch were imaged at $10 \times$ magnification with brightfield microscopy immediately and 7 h (for ECFCs) or 6 h 20 min (for diabetic HMVECs) after scratching. Total scratch area was analyzed using ImageJ (NIH), and % EC migration was calculated as follows:

$$\% \text{ EC migration} = \frac{\text{Total scratch area}_{t=0} - \text{Total scratch area}_{t=h}}{\text{Total scratch area}_{t=0}} * 100$$

We further evaluated the influence of conditioned media from the distinct spheroids on the migratory activity of endothelial cells in 3D using a transwell migration assay. Transwell cell culture 8 μm FluoroBlok^{TM} inserts (Corning, Corning, NY) were coated with 0.1% gelatin. ECFCs were treated with mitomycin C (5 μg/mL) for 30 min. Mitomycin C was replaced with fresh EGM-2$_{non-supp}$. ECFCs were seeded at 1.28×10^5 cells/well in the upper chamber of the culture insert and allowed to settle for 2 h. Media was added to the lower chamber, where fully supplemented EGM-2 was used as a positive control, EGM-2$_{non-supp}$ was the negative control, and experimental groups consisted of 1:1 EGM-2$_{non-supp}$:CM where CM was 100:0, 50:50 (or 1:1), or 0:100 VEGF$_{MAX}$:PGE$_{2,MAX}$ CM. Cells were incubated for 18 h and then stained with calcein AM (2 μM; ThermoFisher) for 30 min. Migration was determined by capturing fluorescence for each well using a Synergy HTX Multimode Reader (Biotek, Winooski, VT).

PGE$_2$ Bioactivity Validation via Scratch Wound Assay

We assessed the bioactivity of secreted PGE$_2$ by scratch wound assays using HaCaTs to determine epithelialization potential of spheroid CM. HaCaTs were seeded in 48-well plates at 4×10^4 cells/well. Cells were cultured for 3 days and treated with mitomycin C (5 μg/mL) for 30 min. Mitomycin C was replaced with fresh culture medium, and cells were uniformly scraped with a 200 μL pipette tip. Following wounding, wells were washed with culture medium to remove any debris, and media was replaced with the respective treatment conditions. Fully supplemented DMEM and 340 pg/mL recombinant PGE$_2$ (rPGE$_2$) were used as positive controls and non-supplemented DMEM was used as the negative control. Experimental groups consisted of 3:1 1% FBS supplemented DMEM:treatment where treatment was 100:0, 50:50 (or 1:1), or 0:100 VEGF$_{MAX}$:PGE$_{2,MAX}$ CM. A mini-

mum of three regions per scratch were imaged at $10 \times$ magnification with brightfield microscopy immediately and 23 h after scratching. Total scratch area was analyzed using ImageJ (NIH) and % HaCaT migration was calculated as follows:

$$\% \text{ HaCaT migration} = \frac{\text{Total scratch area}_{t=0} - \text{Total scratch area}_{t=23h}}{\text{Total scratch area}_{t=0}} * 100$$

PEG-4MAL Hydrogel Synthesis and Spheroid Encapsulation

Four-arm poly(ethylene glycol) (PEG) macromer with maleimide groups at each terminus (PEG-4MAL) (MW 20,000; Laysan Bio, Arab, AL) was dissolved in 4-(2-hydroxyethyl)-1-piperazineethanesulfonic acid) (HEPES) buffer (20 mM in DPBS, pH 7.4). Adhesive and cross-linking peptides were custom synthesized by GenScript (Piscataway, NJ). Adhesive peptide (GRGDSPC, RGD-C, pH 5.5–6) was dissolved in HEPES to generate functionalized PEG-4MAL precursor. Bis-cysteine cross-linking peptide GCRDGPQG↓IAGQDRCG (GPQ-A; ↓ denotes enzymatic cleavage site, pH 4.5 $\pm$ 0.1) was dissolved in HEPES at 1:1 maleimide/cysteine ratio after accounting for maleimide groups reacted with adhesive peptide. RGD-C was polymerized to PEG-4MAL macromer at 37 °C for at least 15 min. Spheroid suspensions were added to the functionalized PEG-4MAL precursor to achieve a final concentration of 5×10^6 cells/mL. Gels were individually synthesized by mixing the PEG-4MAL solution with GPQ-A in 8 mm diameter circular silicone molds.[8] The hydrogels were crosslinked at 37 °C for 20 min to produce 8.0% 20-kDa PEG-4MAL (wt/vol) hydrogels with a final adhesive ligand concentration of 2 mM. Following gelation, the gels were transferred into individual wells of 24-well plates, and the medium was refreshed every 2 days.

Spheroid Response to Hydrogel Formulations

We assessed cell viability by a Live/Dead assay (ThermoFisher). Metabolic activity was determined using an alamarBlue assay (Invitrogen), with fluorescence read at 590 nm. After 1, 4, and 7 days in culture, spheroids were imaged with brightfield microscopy to assess spheroid spreading in the xy-plane of the scaffold. Spreading of cells from the spheroids was evaluated in ImageJ (NIH) by quantifying the number of protrusions from the spheroids and the protrusion lengths by measuring from the center of the spheroid to the leading edge. These data were calculated on a per spheroid basis where a minimum of 3 spheroids per

scaffold were measured and a minimum of 3 scaffolds per group were analyzed. DNA content was measured with the PicoGreen dsDNA assay (Invitrogen).

Statistical Analysis

Data are presented as means ± standard deviation. Data are derived from a minimum of three independent experiments, and the number of experiments is denoted in the figure legends. Statistical significance was assessed by one-way ANOVA with Tukey's multiple comparisons test or Student's t-test when appropriate. p-values < 0.05 were considered statistically significant. Statistical analysis was performed using GraphPad Prism® 9 software (GraphPad Software, San Diego, CA). Significance is denoted by alphabetical letterings. Different letters denote statistical significance between groups, while data sharing a letter are not statistically different from one another.

RESULTS

DOE Reveals Interplay Between Microenvironmental Conditions and MSC Spheroid Response

We used a DOE approach to determine the significance and interaction of spheroid cell number, percentage of ECFCs, and $CoCl_2$ concentration on the secretion of VEGF by MSC spheroids. The secretory potential of the spheroids was dependent on the cell number, percentage of ECs, and $CoCl_2$ concentration (Fig. 1c). Spheroid cell number had a weak quadratic relationship with VEGF secretion while percentage of EC and $CoCl_2$ concentration demonstrated a positive linear relationship with VEGF secretion. The 3D response surface map generated from the model predicted maximum VEGF secretion ($VEGF_{MAX}$) from spheroids with 8000 cells, 0% ECs, and treated with 95.4 μM $CoCl_2$, while minimum VEGF secretion ($VEGF_{MIN}$) from spheroids with 2,850 cells, 66% ECs, and treated with 8.8 μM $CoCl_2$ (Table 1).

Spheroids predicted to distinctly maximize and minimize PGE_2 production were achieved by combining our previously reported work on the optimization of MSC spheroids to enhance anti-inflammatory and proangiogenic potentials and the utilization of co-culture EC-MSC spheroids to enhance capillary network formation.[25] The number of cells per spheroid and Pam3CSK4 concentration markedly influenced PGE_2 secretion. Spheroids predicted to maximize PGE_2 secretion ($PGE_{2,MAX}$) were composed of 60,000 cells and 33% ECs with 1 μg/mL Pam3CSK4, while spheroids predicted to minimize PGE_2 secretion

($PGE_{2,MIN}$) were comprised of 15,000 cells and 33% ECs with 0 μg/mL Pam3CSK4 (Table 2).

The formulations predicted by the DOE models exemplify the tunability of MSC spheroids and demonstrate the interplay of spheroid cell number, percentage of ECs, and $CoCl_2$ or Pam3CSK4 concentration on VEGF or PGE_2 secretion, respectively. By modulating the microenvironmental conditions in a precise manner, we can effectively tune the secretion of pro-regenerative cytokines from MSC spheroids.

Cytokine Secretion by MSC Spheroids is Driven by Microenvironmental Conditions

We measured the secretion of VEGF and PGE_2 to validate DOE formulations predicted to maximize and minimize VEGF and PGE_2 production. $VEGF_{MAX}$ secreted 21.2-fold more normalized VEGF (48 ± 32 pg VEGF/ng DNA) than $VEGF_{MIN}$ (Fig. 2a). We did not observe significant differences in VEGF secretion among $VEGF_{MIN}$, $PGE_{2,MAX}$, and $PGE_{2,MIN}$ spheroids. Furthermore, $PGE_{2,MAX}$ secreted 3.3-fold more PGE_2 (1.3 ± 0.3 pg PGE_2/ng DNA) compared to $PGE_{2,MIN}$ spheroids (Fig. 2b). As expected, $PGE_{2,MAX}$ had significantly elevated PGE_2 secretion compared to the VEGF counterparts. There were no statistical differences in PGE_2 secretion among $PGE_{2,MIN}$, $VEGF_{MAX}$, and $VEGF_{MIN}$ spheroids. Collectively, $VEGF_{MAX}$ spheroids had a 90.3-fold increase in normalized VEGF production compared to $PGE_{2,MAX}$ spheroids, and $PGE_{2,MAX}$ spheroids had a 5.6-fold increase in normalized PGE_2 production compared to $VEGF_{MAX}$ spheroids, validating the formulations extrapolated from the DOEs for these two unique spheroids.

To confirm the reproducibility of these optimized spheroids, we made spheroids from MSCs derived from different donors and measured cytokine secretion. Spheroids made with MSCs from donor 2 (human MSCs from Texas A&M) achieved similar secretion levels as spheroids made with MSCs from donor 1 (human MSCs from RoosterBio) (Supplementary Fig. S1). These data emphasize that the interplay of spheroid cell number, percentage of ECs, and treatment are donor independent and confirm the reproducibility of the formulations identified by the DOE.

We further characterized the secretome profiles of $VEGF_{MAX}$ and $PGE_{2,MAX}$ spheroids (Fig. 2c). Of the analytes examined, the $VEGF_{MAX}$ secretome was primarily composed of VEGF-A, with EGF and HGF and trace amounts of the other analytes. On the other hand, the $PGE_{2,MAX}$ secretome was composed predominantly of CD31, followed by TIE-2, EGF, HGF, and follistatin. $VEGF_{MAX}$ spheroids contained 30-fold
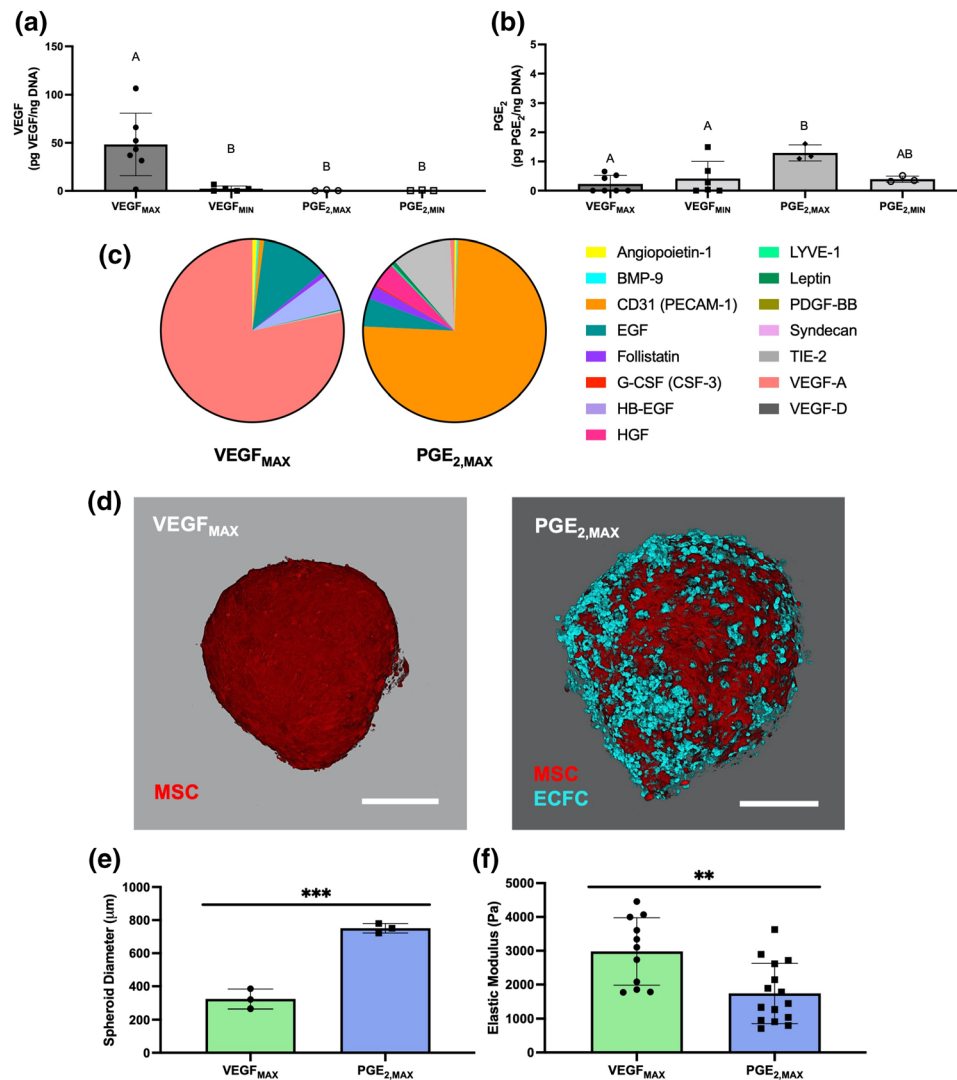
FIGURE 2. Validation of the DOE model examining cytokine production by the distinct spheroids, and morphological and mechanical characterization of $VEGF_{MAX}$ and $PGE_{2,MAX}$ spheroids. (a) Total VEGF secretion and (b) total PGE_2 secretion normalized to total DNA content from spheroid formulations predicted to maximize VEGF ($VEGF_{MAX}$) or PGE_2 ($PGE_{2,MAX}$) and minimize VEGF ($VEGF_{MIN}$) or PGE_2 ($PGE_{2,MIN}$) ($n = 3$–6). (c) Cytokine content in the secretome of $VEGF_{MAX}$ and $PGE_{2,MAX}$ spheroids. (d) Representative $VEGF_{MAX}$ and $PGE_{2,MAX}$ spheroids with ECs (cyan) and MSCs (red) at 48 h post-spheroid formation as observed by confocal microscopy. Scale bars are 200 μm. (e) Spheroid diameter ($n = 3$) and (f) elastic modulus ($n = 11$–15) of $VEGF_{MAX}$ and $PGE_{2,MAX}$ spheroids at 48 h post-spheroid formation. Significance is denoted by alphabetical letterings or asterisks where different letters ($p < 0.05$) or ** ($p < 0.01$) and *** ($p < 0.001$).

more VEGF-A (4098 ± 2490 pg/mL) compared to $PGE_{2,MAX}$ spheroids (136 ± 21 pg/mL). $PGE_{2,MAX}$ spheroids had 293-fold, 129-fold, 2.3-fold, and 1.5-fold more CD31, TIE-2, HGF, and EGF secretion compared to $VEGF_{MAX}$ spheroids, respectively. These data emphasize the different secretory profiles of the distinct spheroid formulations.

$VEGF_{MAX}$ and $PGE_{2,MAX}$ Spheroids Have Unique Morphologies and Cell Distributions

Following the validation of the predicted formulations, we focused on two spheroids of interest –

$VEGF_{MAX}$ and $PGE_{2,MAX}$. After 48 h of spheroid formation, $VEGF_{MAX}$ spheroids appeared slightly elliptical in morphology with tight cell compaction while $PGE_{2,MAX}$ spheroids exhibited a rounder morphology with a close-knit cell arrangement (Fig. 2d). Interestingly, ECs in $PGE_{2,MAX}$ spheroids were unevenly dispersed among the MSCs in the spheroid but were congregated together as multiple cell clusters. $PGE_{2,MAX}$ spheroid diameter was 2.3-fold larger than $VEGF_{MAX}$ spheroids, measuring 750.9 ± 28.6 μm vs. 323.6 ± 59.9 μm (Fig. 2e). The elastic modulus of $VEGF_{MAX}$ spheroids (3674 ± 1924 Pa) was 2.1-fold greater than

$PGE_{2,MAX}$ spheroids (1741 ± 887 Pa), a fold increase inversely related to the diameter size (Fig. 2f). Further investigation is merited to explore whether this relationship is due to the difference in spheroid diameter or EC incorporation.

Functionally Distinct MSC Spheroids Secrete Bioactive Cytokines that Promote EC Migration

We next characterized the functional bioactivity of secreted proangiogenic growth factors by testing the ability of spheroid conditioned media (CM) to stimulate ECFC migration (Fig. 3a). ECFCs were treated with CM from $VEGF_{MAX}$, $PGE_{2,MAX}$, or a combination at a 1:1 ratio. ECFCs in the negative control (0.4 ± 3.5% ECFC migration) exhibited limited migration and receded from the leading edge of the initial scratch, taking on a more rounded morphology (Fig. 3a). In contrast, ECFCs stimulated with CM from $VEGF_{MAX}$ spheroids (22.4 ± 1.6% ECFC migration) demonstrated robust migration, exhibiting 1.3-fold more migration than ECFCs stimulated with CM from $PGE_{2,MAX}$ spheroids (16.6 ± 1.5% ECFC migration) (Fig. 3b). CM composed of a combination of 1:1 $VEGF_{MAX}$ to $PGE_{2,MAX}$ CM (19.0 ± 1.7% ECFC migration) promoted migration at intermediate levels, suggesting the combined CM acts on the ECFCs in an additive manner. $VEGF_{MAX}$ CM treated groups demonstrated less migration compared to the EGM-2 treated (35.4 ± 1.3% ECFC migration) but exhibited 1.4-fold more migration compared to groups treated with rVEGF (16.0 ± 0.8% ECFC migration). These data confirm the functional bioactivity of secreted proangiogenic growth factors from $VEGF_{MAX}$ spheroids. In addition to VEGF, the secretome of $VEGF_{MAX}$ spheroids contains an array of cytokines that act in concert to promote the robust migration of ECFCs.

We also evaluated the migratory response of ECFCs to spheroid CM using a transwell migration assay (Supplementary Fig. S2). CM from $VEGF_{MAX}$ (1039 ± 206 RFU) and $PGE_{2,MAX}$ (1003 ± 239 RFU) induced nearly 5-fold more ECFC migration compared to the negative control, with cell migration similar to the positive control. Unlike in the scratch migration assay, we did not observe significant differences in ECFC migration among groups treated with $VEGF_{MAX}$ and $PGE_{2,MAX}$ CM. This behavior could be attributed to the nature of this assay. Transwell migration assays require low concentrations of chemoattractants to induce migration through the permeable filter. VEGF is a key stimulator of endothelial cell migration during angiogenesis along with other cytokines such as HGF and EGF. $VEGF_{MAX}$ CM contained high levels of VEGF with some HGF and EGF, while $PGE_{2,MAX}$ CM also contained HGF and EGF (Fig. 2c). These data suggest the presence of HGF and EGF in $PGE_{2,MAX}$ CM was sufficient to promote ECFC migration in the transwell.

In chronic wounds, ECs are dysfunctional and unresponsive to potent bioactive factors. To investigate the potency of the spheroid secretomes on rescuing the responsiveness and functionality of ECs from chronic wounds, we tested the effects of our spheroid CM on the migration of diabetic HMVECs (Fig. 3c). Diabetic HMVECs treated with $VEGF_{MAX}$ CM (26.8 ± 4.8% diabetic HMVEC migration) migrated 1.3-fold more than diabetic HMVECs treated with $PGE_{2,MAX}$ CM (20.6 ± 4.3% diabetic HMVEC migration) (Fig. 3d). Combined $VEGF_{MAX}$ and $PGE_{2,MAX}$ CM (23.8 ± 1.9% diabetic HMVEC migration) displayed an additive effect on migration. While not significant, $VEGF_{MAX}$ CM induced more migration than EGM-MV2 (26.1 ± 5.2% diabetic HMVEC migration). Similar to ECFCs, diabetic HMVECs migrated more when treated with $VEGF_{MAX}$ CM compared to rVEGF (20.3 ± 3.9% diabetic HMVEC migration). Collectively, diabetic HMVECs did not exhibit notable differences in migration among groups treated with various CM ratios and rVEGF. However, they did demonstrate similar, although more muted, behavioral trends as the ECFCs, which was anticipated given the impaired functionality of diabetic HMVECs. These findings indicate that $VEGF_{MAX}$ spheroids can partially rescue the functionality of diabetic HMVECs.

Functionally Distinct MSC Spheroids Secrete Bioactive Cytokines That Promote Epithelialization

To characterize the bioactivity of secreted cytokines to promote epithelialization, we tested the ability of spheroid CM to induce HaCaT cell migration (Fig. 4a). HaCaTs were treated with CM from $VEGF_{MAX}$, $PGE_{2,MAX}$, or a combination at a 1:1 ratio. CM from $PGE_{2,MAX}$ spheroids (29.0 ± 2.5% HaCaT migration) induced 1.3-fold more HaCaT migration compared to CM from $VEGF_{MAX}$ spheroids (22.6 ± 3.8% HaCaT migration) (Fig. 4b). The addition of CM from $PGE_{2,MAX}$ spheroids to the CM from $VEGF_{MAX}$ spheroids in the 1:1 $VEGF_{MAX}$:$PGE_{2,MAX}$ (27.5 ± 3.9% HaCaT migration) rescued the migration of HaCaTs. $PGE_{2,MAX}$ CM promoted significantly more HaCaT migration compared to the fully supplemented DMEM positive control while the negative control (6.5 ± 2.3% HaCaT
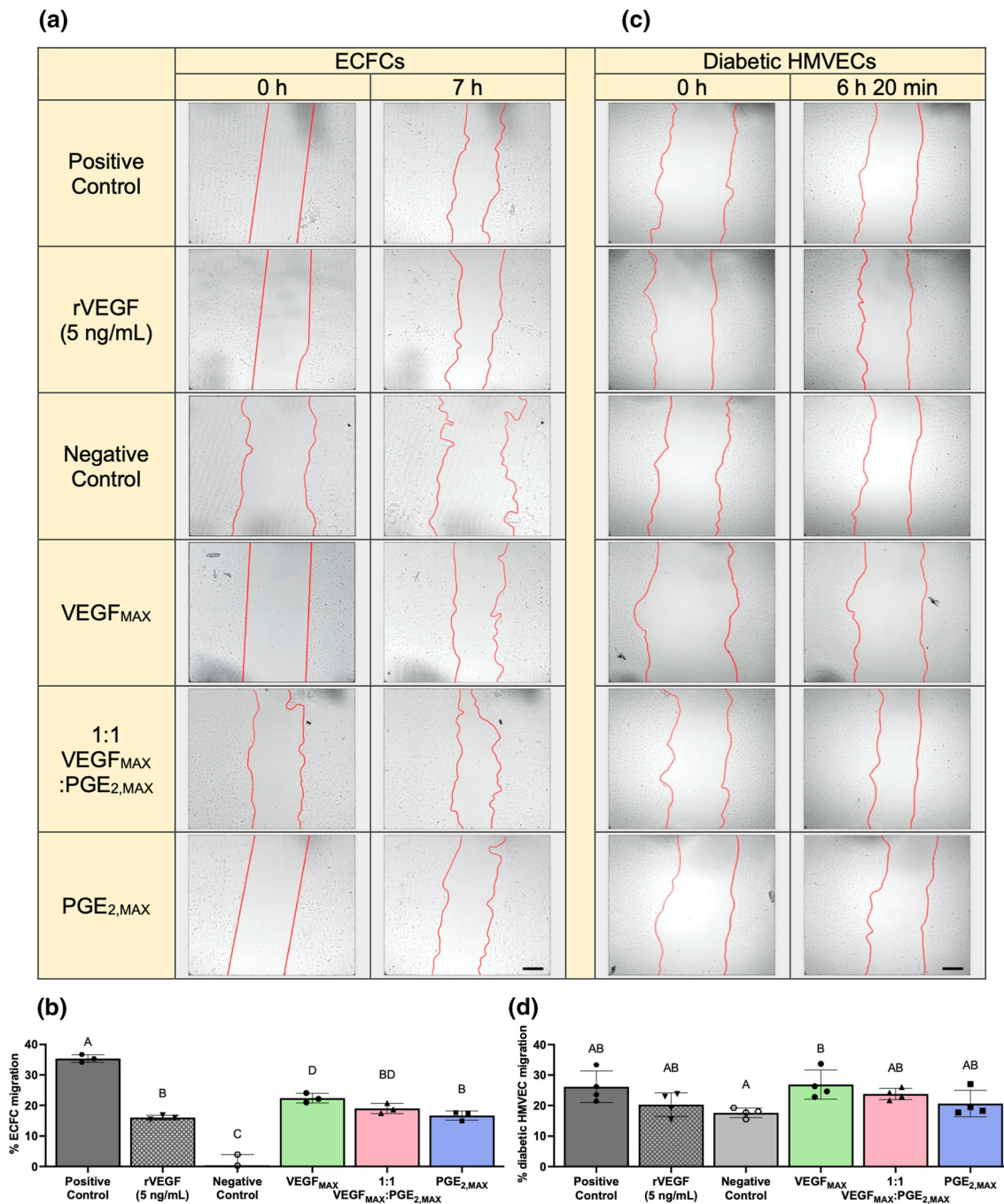
FIGURE 3. VEGF$_{MAX}$ spheroids secrete bioactive cytokines that enhance EC migration. Images of (a) ECFCs and (c) diabetic HMVECs in scratch migration assay before and after treatment with CM from VEGF$_{MAX}$, 1:1 VEGF$_{MAX}$:PGE$_{2,MAX}$, PGE$_{2,MAX}$, and 5 ng/ mL rVEGF for 7 h or 6 h 20 min, respectively. Fully supplemented and non-supplemented media were used as a positive and negative control, respectively. Red lines indicate the leading edges of the scratch. Scale bars are 200 μm. (b) Quantification of % ECFC migration at 7 h (n = 3) and (d) % diabetic HMVEC migration (n = 4) at 6 h 20 min post-scratch and treatment. Different letters denote statistical significance ($p < 0.05$).

migration) induced limited migration. Intriguingly, HaCaTs treated with rPGE$_2$ (11.06 $\pm$ 2.60% HaCaT migration) exhibited 2.6-fold less migration compared to PGE$_{2,MAX}$ CM, suggesting that there are other important components in PGE$_{2,MAX}$ CM that jointly promote epithelialization.

Paracrine Signaling Induces Cellular Protrusions from Spheroids in MMP-Degradable PEG-4MAL Hydrogels

VEGF$_{MAX}$ and PGE$_{2,MAX}$ spheroids were encapsulated in PEG-4MAL hydrogels to study their

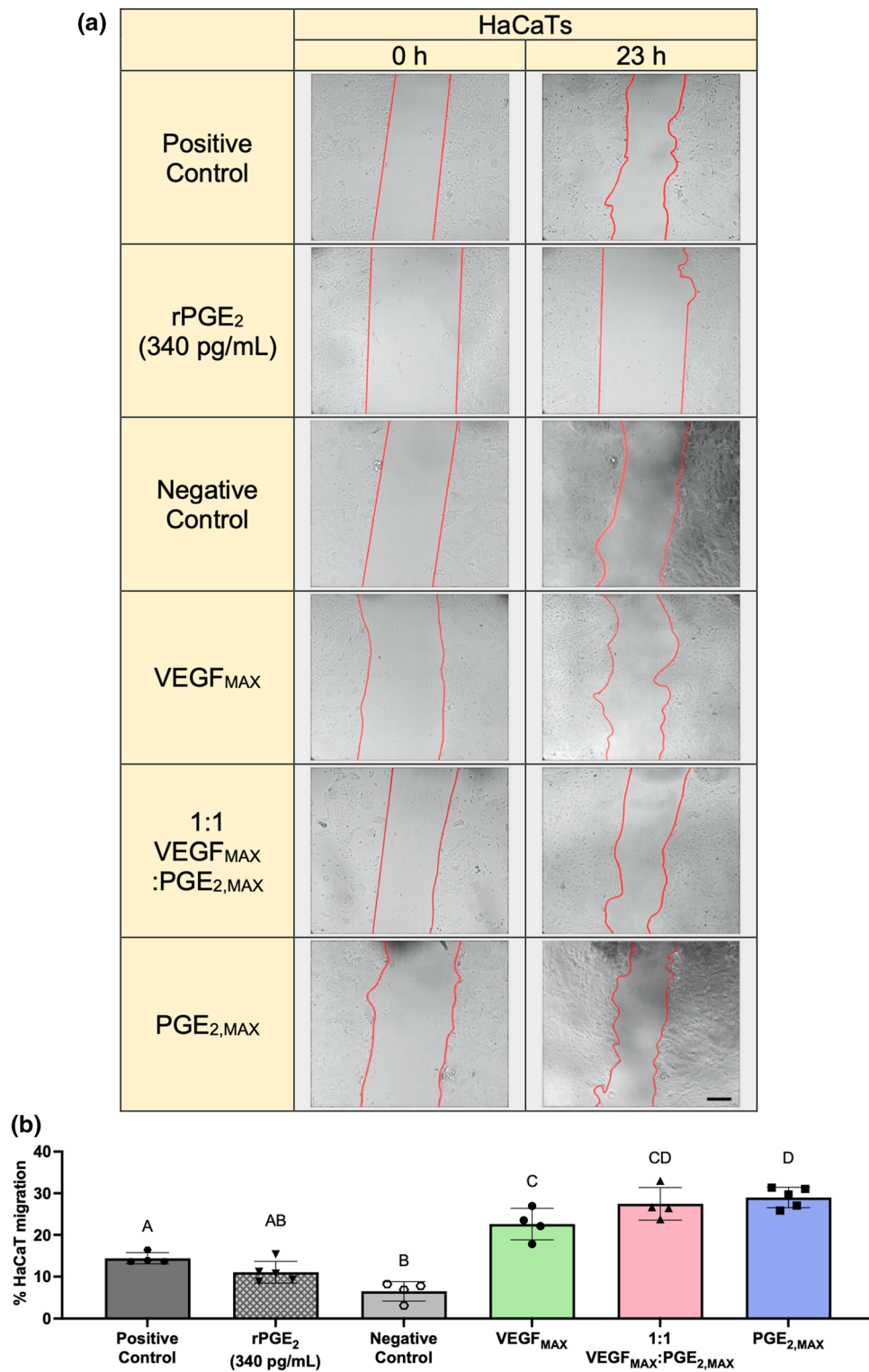**BMES** BIOMEDICAL ENGINEERING SOCIETY

FIGURE 4. $PGE_{2,MAX}$ spheroids secrete bioactive cytokines that promote keratinocyte migration. (a) Images of HaCaTs in scratch wound assay before and after treatment with CM from $VEGF_{MAX}$, 1:1 $VEGF_{MAX}:PGE_{2,MAX}$, $PGE_{2,MAX}$, and 340 pg/mL $rPGE_2$ for 23 h. Red lines indicate the leading edges of the scratch. Scale bars are 200 μm. (b) Quantification of % HaCaT migration at 23 h post-scratch and treatment ($n = 4$). Different letters denote statistical significance ($p < 0.05$).

BMES BIOMEDICAL ENGINEERING SOCIETY
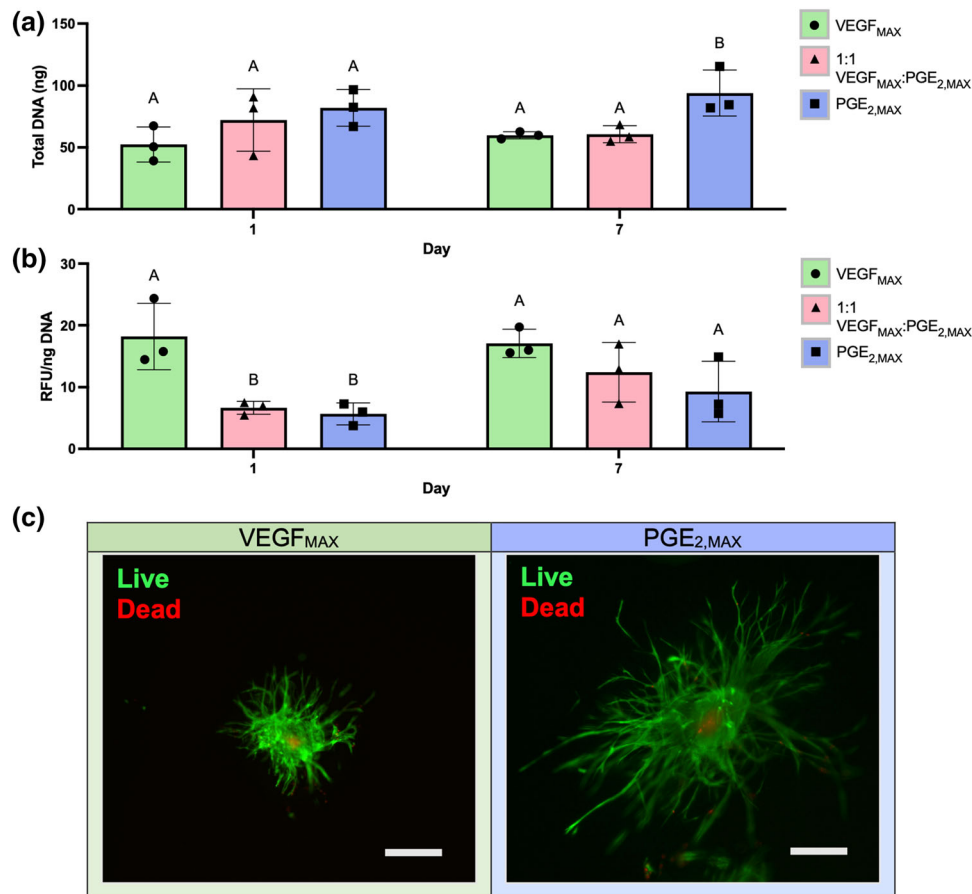
FIGURE 5. Interaction of functionally distinct spheroids in MMP-sensitive PEG-4MAL hydrogels. (a) Total DNA content and (b) metabolic activity of spheroids in PEG-4MAL gels on days 1 and 7 ($n = 3$). Statistical analysis was conducted between groups within each time point. Different letters denote statistical significance ($p < 0.05$). (c) Live (green)/dead (red) assay showing the viability of $VEGF_{MAX}$ and $PGE_{2,MAX}$ in 8% PEG-4MAL at day 7. Spheroids were seeded at a ratio of 1:1 $VEGF_{MAX}$:$PGE_{2,MAX}$ spheroids. Scale bar represents 200 μm.

behavior in a 3D environment. Gels contained either $VEGF_{MAX}$ spheroids, $PGE_{2,MAX}$ spheroids, or 1:1 ratio of $VEGF_{MAX}$:$PGE_{2,MAX}$ spheroids. DNA content remained relatively flat over 7 days for each spheroid ratio (Fig. 5a), suggesting MSCs and ECFCs are not proliferating dramatically over the study duration. On day 1, all groups had similar levels of DNA, ranging between 50 and 85 ng of total DNA. However, on day 7, we detected a 1.6-fold increase in total DNA for gels with only $PGE_{2,MAX}$ spheroids (94.0 ± 18.5 ng DNA) compared to gels with only $VEGF_{MAX}$ (59.8 ± 2.8 ng DNA) or 1:1 $VEGF_{MAX}$:$PGE_{2,MAX}$ (60.7 ± 6.9 ng DNA) spheroids. Similar to DNA content, metabolic activity was consistent over 7 days for each spheroid ratio (Fig. 5b). On day 1, gels with only $VEGF_{MAX}$ spheroids displayed a 2.9-fold increase in metabolic activity compared to $PGE_{2,MAX}$ only (5.7 ± 1.8 RFU/ng DNA) and 1:1 $VEGF_{MAX}$:$PGE_{2,MAX}$ (6.6 ± 1.1 RFU/ng DNA) groups. There were no significant differences among the groups on day 7, although there appeared

to be an increase in metabolic activity as the number of $VEGF_{MAX}$ spheroids was increased. These data suggest that $PGE_{2,MAX}$ spheroids proliferated more in PEG-4MAL hydrogels by day 7 compared to other groups, which could be attributed to the MSCs acting on and promoting the proliferation of neighboring ECFCs in the $PGE_{2,MAX}$ spheroid. $VEGF_{MAX}$ only containing gels exhibited a burst in metabolic activity at day 1. This increase may result from an increased energy expenditure by cells to adhere and spread into the gel, as $VEGF_{MAX}$ exhibited a 1.7-fold larger elastic modulus compared to $PGE_{2,MAX}$ spheroids (Fig. 2f).

To investigate cell viability in PEG-4MAL gels, we performed a live/dead stain on spheroids seeded at 1:1 ratio of $VEGF_{MAX}$:$PGE_{2,MAX}$. We confirmed a hypoxic core was not present in $PGE_{2,MAX}$ spheroids due to their large spheroid diameter (Fig. 2e). After 7 days in culture, $VEGF_{MAX}$ and $PGE_{2,MAX}$ entrapped spheroids exhibited similar viability (Fig. 5c), with both spheroid types demonstrating changes in morphology as cells migrated into the gel. Cells in
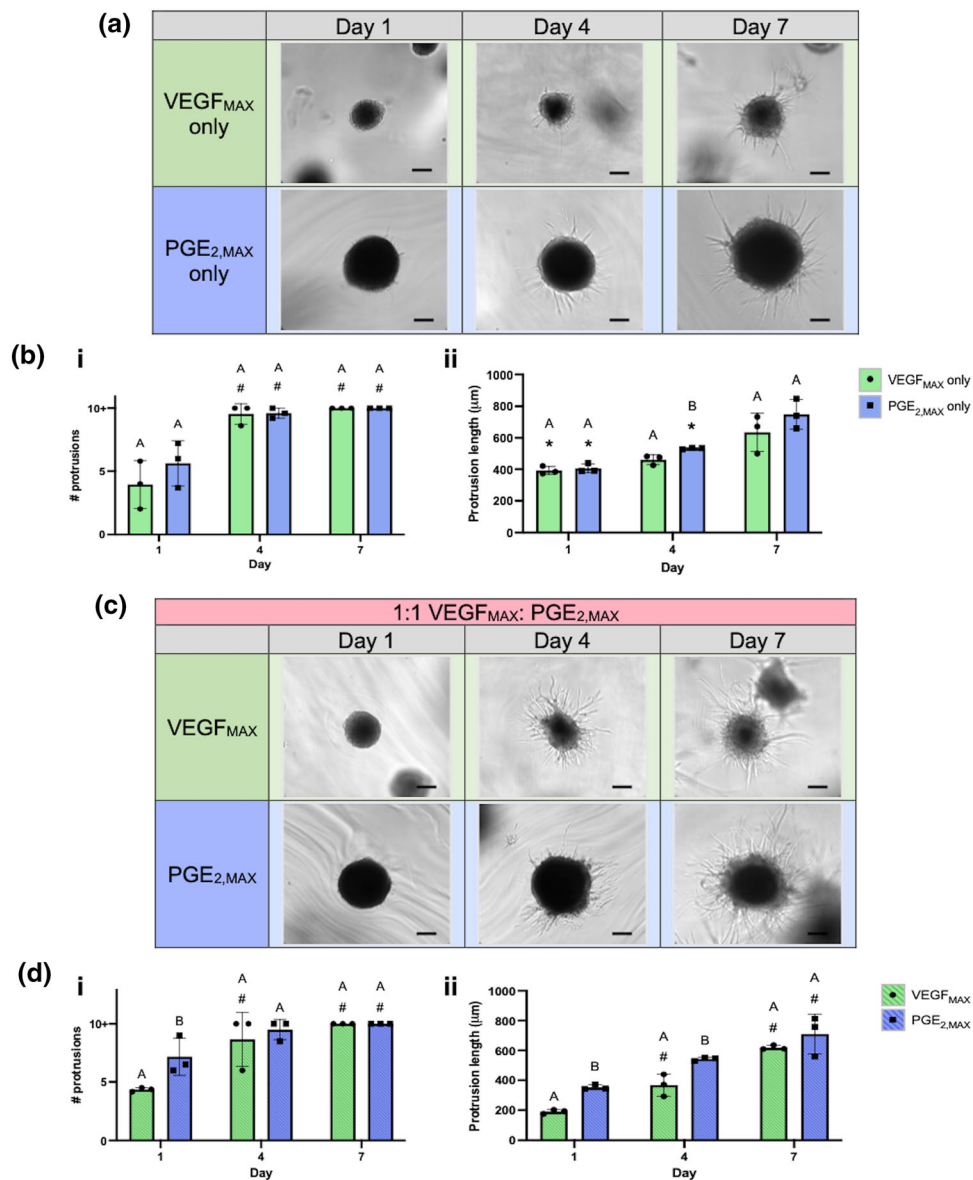
FIGURE 6. Influence of distinct spheroids on cell spreading in MMP-sensitive PEG-4MAL hydrogels. (a) Brightfield images of cell spreading and (b) number of protrusions (i) and protrusion length (ii) from $VEGF_{MAX}$ and $PGE_{2,MAX}$ spheroids in gels seeded with only $VEGF_{MAX}$ or $PGE_{2,MAX}$ spheroids on days 1, 4, and 7 ($n = 3$). (c) Brightfield images of cell spreading and (d) number of protrusions (i) and protrusion length (ii) from $VEGF_{MAX}$ and $PGE_{2,MAX}$ spheroids in gels loaded with spheroids at 1:1 $VEGF_{MAX}$:$PGE_{2,MAX}$ on days 1, 4, and 7 ($n = 3$). * indicates significant differences between that group and day 7 of the same group ($p < 0.05$). # indicates significant differences between that group and day 1 of the same group ($p < 0.05$). Different letters denote statistical differences between groups on designated days ($p < 0.05$). Scale bars represent 200 μm.

$PGE_{2,MAX}$ spheroids migrated rapidly into the surrounding matrix, developing long, spindle-like protrusions from the spheroid center. The cells were viable with minimal dead cells in the spheroid. Spreading was also prominent, although not as extensive as the cells in the $PGE_{2,MAX}$ spheroids. In these studies, we chose day 7 to assess cellular sprouting during the onset of the proliferation stage. By day 7 of the wound healing cascade, inflammation in the wound bed is typically resolved and proliferation has begun (*i.e.*, ECs and keratinocytes are recruited for angiogenesis and epithelialization, respectively). Future work to study cellular behavior on day 14 would capture spheroid function at later stages in the wound healing cycle.

The MMP-sensitivity of the PEG-4MAL hydrogels facilitates gel degradation by spheroid-secreted MMPs, providing a scaffold to investigate the interaction of the unique MSC spheroids with their microenviron-

ment. We assessed cell spreading from the spheroids in the gels by quantifying the number of protrusions and the protrusion lengths (Fig. 6b i,ii). On day 1, $PGE_{2,MAX}$ spheroids exhibited 1.4-fold more protrusions than $VEGF_{MAX}$ spheroids, with no differences in protrusion lengths (390–410 μm) (Fig. 6a). However, on day 4, we observed the opposite trend with no apparent distinctions in the number of protrusions but significant differences in protrusion length-$PGE_{2,MAX}$ spheroids (532 ± 5 μm) had 1.2-fold longer protrusions compared to $VEGF_{MAX}$ spheroids (461 ± 31 μm). This behavior was maintained on day 7 when the number of protrusions for $VEGF_{MAX}$ only and $PGE_{2,MAX}$ only hydrogel groups exceeded 10 and $PGE_{2,MAX}$ (750 ± 94 μm) had 1.2-fold longer protrusions compared to $VEGF_{MAX}$ (635 ± 121 μm). For both groups, the number of protrusions and protrusion length increased over 7 days. These data demonstrate that PEG-4MAL scaffolds enable cellular protrusions from $VEGF_{MAX}$ and $PGE_{2,MAX}$ spheroids, evidenced by the increasing number of protrusions and protrusion length over time.

To examine the influence of spheroid type on cell spreading, we quantified protrusion number and protrusion length from $VEGF_{MAX}$ and $PGE_{2,MAX}$ spheroids when seeded at 1:1 ratio of $VEGF_{MAX}$:$PGE_{2,MAX}$ spheroids in PEG-4MAL hydrogels (Fig. 6d i,ii). Over 7 days, the number of protrusions and protrusion length increased for both $VEGF_{MAX}$ and $PGE_{2,MAX}$ spheroids (Fig. 6c). $PGE_{2,MAX}$ spheroids (353 ± 16 μm, day 1; 543 ± 12 μm, day 4) had significantly longer protrusions than $VEGF_{MAX}$ spheroids (191 ± 13 μm, day 1; 368 ± 74 μm, day 4), which plateaued by day 7. Interestingly, the combination of the two distinct spheroids increased the number of protrusions on day 1 in $VEGF_{MAX}$ spheroids by 1.1-fold and $PGE_{2,MAX}$ spheroids by 1.3-fold more compared to the respective spheroids in the $VEGF_{MAX}$ only or $PGE_{2,MAX}$ only gels while the protrusion length remained unaffected. These differences were less apparent by day 4 and 7 for both spheroid types. Together, these data suggest that increases in protrusion number for each unique spheroid on day 1 is related to paracrine signaling between the spheroids.

DISCUSSION

MSCs are widely studied to promote wound healing and tissue regeneration due to their abundant therapeutic potential and their potent secretomes.[1,19] We and others previously reported the development of MSC spheroids that enhance VEGF and PGE_2 production compared to MSCs cultured in mono-

layer.[21,25,37] However, this approach is limited by the dependence on host ECs for neovascularization, posing a challenge as ECs in chronic, nonhealing wounds are unresponsive to potent bioactive factors in their environment.[10] Furthermore, the simultaneous induction of VEGF and PGE_2 secretion from a single spheroid inhibits the ability to fully capitalize on the therapeutic capabilities of MSCs. In this study, we addressed these challenges by engineering MSC spheroids with distinct therapeutic potentials (*i.e.*, maximizing VEGF or PGE_2 secretion) and incorporating ECFCs to promote vascularization and epithelialization for wound repair without dependence on native ECs.

This study established that the distinct MSC spheroids possess unique bioactive functionalities. Using DOE, three microenvironmental conditions were tuned to engineer MSC spheroids with various VEGF ($VEGF_{MAX}$ and $VEGF_{MIN}$) or PGE_2 ($PGE_{2,MAX}$ and $PGE_{2,MIN}$) secretion levels. The input variables (*i.e.*, number of cells per spheroid, percentage of ECFCs, and $CoCl_2$ or Pam3CSK4 concentration) were chosen due to their ability to modulate the secretome of MSC spheroids.[25,31,34,35] Spheroid cell number had a weak quadratic relationship with VEGF secretion while percentage of ECs and $CoCl_2$ concentration had a positive linear influence on VEGF levels. On the other hand, PGE_2 secretion levels increased with spheroid cell number and Pam3CSK4 concentration. Using a multiplex cytokine assay, we further characterized the spheroid secretome and established the unique profile compositions of the optimized formulations. Interestingly, CM from either $VEGF_{MAX}$ or $PGE_{2,MAX}$ spheroids promoted more migration than the respective recombinant cytokines when applied to ECFCs, diabetic HMVECs, or HaCaTs in a scratch migration/wound assay. Taken together, these data confirm that the CM from $VEGF_{MAX}$ and $PGE_{2,MAX}$ spheroids is comprised of not only VEGF or PGE_2, respectively, but rather a cocktail of potent factors that work synergistically to enhance angiogenesis and epithelialization. These data also highlight the capability of leveraging the spheroids in a modular fashion.

The cell density of the $PGE_{2,MAX}$ spheroids (60 k cells/spheroid) represents a potential limitation with this approach. When applied clinically, the number of spheroids would need to be scaled up, which could be challenging given the number of MSCs required. We also recognize that other environmental factors (*e.g.*, physiological oxygen tension in the skin) influence the behavior of MSC spheroids, which merits further investigation. Non-steroidal anti-inflammatory drugs (NSAIDs) block cyclooxygenase, which inhibit PGE_2 production. Further exploration is necessary to better

understand the effects of NSAIDs on the therapeutic potential of $PGE_{2,MAX}$ spheroids, as the clinical translation of this approach may coincide with NSAID use. Nonetheless, we demonstrated that we can selectively upregulate the production of specific cytokines in different MSC spheroids using a DOE approach. Furthermore, by independently tuning MSC spheroids, we facilitated paracrine interaction and spheroid crosstalk for therapeutic applications.

MMPs play a critical role in regulating extracellular matrix (ECM) degradation and deposition that is required for epithelialization during cutaneous wound healing.[27] However, chronic wounds are often characterized by an excess amount of MMPs that dysregulate the balance between granulation tissue formation and re-epithelialization.[4] Furthermore, MSC spheroids exhibit increased MMP secretion that facilitates cell spreading and migration.[7] We investigated the interaction of the distinct spheroids using an MMP-degradable PEG-based platform based on its high cytocompatibility and minimal inflammation *in vivo*. PEG-4MAL gels are well characterized and facilitate robust cellular engraftment and growth.[11,26] In addition, the synthetic nature of PEG-4MAL enables high mechanical tunability and the incorporation of elements characteristic of natural ECM, such as cell-adhesion motifs and sites vulnerable to proteases to regulate matrix remodeling during wound healing, which are more difficult to control with natural biomaterials. Overall, the ease of manipulating PEG-4MAL hydrogels is advantageous when considering this platform for clinical translation. PEG-4MAL scaffold degradation can be regulated by tuning the concentration of protease susceptible peptides to facilitate matrix remodeling and accelerate wound healing. $VEGF_{MAX}$ and $PGE_{2,MAX}$ spheroids in PEG-4MAL scaffolds maintained viability over 7 days. There was a burst in metabolic activity at day 1 for hydrogels loaded with only $VEGF_{MAX}$ spheroids and more pronounced proliferative activity for groups containing $PGE_{2,MAX}$ spheroids ($PGE_{2,MAX}$ and 1:1 $VEGF_{MAX}$:$PGE_{2,MAX}$ groups). The burst in metabolic activity at day 1 for gels loaded with only $VEGF_{MAX}$ spheroids may be due to the size and elastic modulus of the spheroids. $VEGF_{MAX}$ spheroids are 43% smaller in diameter and possess a 2.1-fold greater elastic modulus compared to $PGE_{2,MAX}$ spheroids. The more compact size and greater cell–cell adhesion in the $VEGF_{MAX}$ spheroid would require more effort from the MSCs to attach and spread into the surrounding scaffold. This is supported by the smaller number of cell protrusions for $VEGF_{MAX}$ spheroids compared to $PGE_{2,MAX}$ spheroids. MSCs have potent secretomes that act on neighboring cells. Due to their proximity and potential cell interactions between the ECs and

MSCs in $PGE_{2,MAX}$ spheroids, the observed increase in DNA content using these spheroids may be attributed to EC proliferation.[3] In these studies, measurements of cellular protrusions were performed on individual z-planes, which restricted our evaluation to two dimensions. Future work could include capturing the cellular protrusions in the z-direction to assess radial spreading and characterize the direction and alignment of cellular outgrowth.

Current cellular or pharmacological approaches for wound healing are limited because they fail to consider the range of clinical challenges in chronic wounds (*e.g.*, angiogenesis, epithelialization, and regulation of matrix remodeling).[5,22] Herein, we developed a clinically relevant approach using functionally distinct MSC spheroids and established their effectiveness at promoting angiogenesis and epithelialization. The development of functionally distinct MSC spheroids offers the potential to apply them in a modular fashion. However, when used together, the unique spheroids have a positive interaction as demonstrated by the initial elevated number of cell protrusions. Future studies are warranted to investigate the role of MSC spheroid ratio on wound repair. Furthermore, we loaded the MSC spheroids into a biocompatible, highly tunable PEG-4MAL hydrogel to provide a controlled environment to investigate cell attachment and spreading. We utilized a slow-degrading PEG-4MAL gel formulation because we sought to understand the microenvironmental and spheroid-spheroid interactions of our functionally distinct spheroids. Future work to study the influence of gels with varying degradation rates would advance our knowledge on how matrix remodeling impacts cutaneous wound repair. In addition, the application of $VEGF_{MAX}$ and $PGE_{2,MAX}$ spheroids to an *ex vivo* or *in vivo* wound model would deepen our understanding of the therapeutic benefits of these spheroids, but this is beyond the scope of the present work.

We engineered functionally distinct MSC spheroids to promote angiogenesis or epithelialization by maximizing VEGF or PGE_2 secretion, respectively. These MSC spheroids represent an innovative strategy to leverage the unique functionality of spheroids in a modular fashion for the treatment of cutaneous wounds or other tissue deficits. This approach, for the first time, incorporates ECs as building blocks to facilitate vascularization without dependence on host ECs. Collectively, $VEGF_{MAX}$ and $PGE_{2,MAX}$ spheroids deployed in an MMP-degradable PEG-4MAL hydrogel hold promise as a safe, effective treatment for wound healing or other clinical challenges that require effective neovascularization.

BMES BIOMEDICAL ENGINEERING SOCIETY

SUPPLEMENTARY INFORMATION

The online version contains supplementary material available at https://doi.org/10.1007/s10439-023-03162-9.

ACKNOWLEDGMENTS

AUTHOR CONTRIBUTIONS

VLT: conception and design, financial support, collection and/or assembly of data, data analysis and interpretation, manuscript writing, and final approval of manuscript. DOC: collection and/or assembly of data, and final approval of manuscript. JKL: conception and design, financial support, data analysis and interpretation, manuscript writing, final approval of manuscript, and scientific advisor.

DATA AVAILABILITY

The datasets generated during and/or analyzed during the current study are available from the corresponding author on reasonable request.

CONFLICT OF INTEREST

The authors have no conflicts of interest.

OPEN ACCESS

REFERENCES

[1] Ahangar, P., S. J. Mills, and A. J. Cowin. Mesenchymal stem cell secretome as an emerging cell-free alternative for improving wound repair. *Int. J. Mol. Sci.* 21(19):5, 2020.

[2] An, Y., W. J. Liu, P. Xue, Y. Ma, L. Q. Zhang, B. Zhu, et al. Autophagy promotes msc-mediated vascularization in cutaneous wound healing via regulation of vegf secretion. *Cell Death Dis.* 9(2):58, 2018.

[3] Bussche, L., and G. R. Van de Walle. Peripheral blood-derived mesenchymal stromal cells promote angiogenesis via paracrine stimulation of vascular endothelial growth factor secretion in the equine model. *Stem Cells Transl. Med.* 3(12):1514–1525, 2014.

[4] Caley, M. P., V. L. Martins, and E. A. O'Toole. Metalloproteinases and wound healing. *Adv. Wound Care (New Rochelle)*. 4(4):225–234, 2015.

[5] Chen, A., H. He, G. Ma, Y. Li, S. Jiang, X. Xuan, et al. Biodegradable copolypeptide hydrogel prodrug accelerates dermal wound regeneration by enhanced angiogenesis and epithelialization. *RSC Adv.* 8(19):10620–10626, 2018.

[6] Chen, W., X. Liu, Q. Chen, C. Bao, L. Zhao, Z. Zhu, et al. Angiogenic and osteogenic regeneration in rats via calcium phosphate scaffold and endothelial cell co-culture with human bone marrow mesenchymal stem cells (mscs), human umbilical cord mscs, human induced pluripotent stem cell-derived mscs and human embryonic stem cell-derived mscs. *J. Tissue Eng. Regen. Med.* 12(1):191–203, 2018.

[7] Cheng, N. C., S. Y. Chen, J. R. Li, and T. H. Young. Short-term spheroid formation enhances the regenerative capacity of adipose-derived stem cells by promoting stemness, angiogenesis, and chemotaxis. *Stem Cells Transl. Med.* 2(8):584–594, 2013.

[8] Cruz-Acuna, R., M. Quiros, S. Huang, D. Siuda, J. R. Spence, A. Nusrat, et al. PEG-4MAL hydrogels for human organoid generation, culture, and in vivo delivery. *Nat. Protoc.* 13(9):2102–2119, 2018.

[9] Deng, B., X. Zhang, Y. Liang, H. Jiang, W. Huang, Y. Wu, et al. Nonadherent culture method promotes msc-mediated vascularization in myocardial infarction via mir-519d/vegfa pathway. *Stem Cell Res. Ther.* 11(1):266, 2020.

[10] Ding, H., and C. R. Triggle. Endothelial cell dysfunction and the vascular complications associated with type 2 diabetes: assessing the health of the endothelium. *Vasc. Health Risk Manag.* 1(1):55–71, 2005.

[11] Enemchukwu, N. O., R. Cruz-Acuna, T. Bongiorno, C. T. Johnson, J. R. Garcia, T. Sulchek, et al. Synthetic matrices reveal contributions of ecm biophysical and biochemical

properties to epithelial morphogenesis. *J. Cell Biol.* 212(1):113–124, 2016.

[12]Gionet-Gonzales, M. A., and J. K. Leach. Engineering principles for guiding spheroid function in the regeneration of bone, cartilage, and skin. *Biomed Mater.*13(3):034109, 2018.

[13]Gonzalez-Fernandez, T., A. J. Tenorio, A. M. Saiz Jr., and J. K. Leach. Engineered cell-secreted extracellular matrix modulates cell spheroid mechanosensing and amplifies their response to inductive cues for the formation of mineralized tissues. *Adv. Healthc. Mater.*11(10):e2102337, 2022.

[14]Griffin, K. H., S. W. Fok, and J. K. Leach. Strategies to capitalize on cell spheroid therapeutic potential for tissue repair and disease modeling. *NPJ. Regen. Med.* 7(1):70, 2022.

[15]Harvestine, J. N., T. Gonzalez-Fernandez, A. Sebastian, N. R. Hum, D. C. Genetos, G. G. Loots, et al. Osteogenic preconditioning in perfusion bioreactors improves vascularization and bone formation by human bone marrow aspirates. *Sci. Adv.* 6(7):eaay2387, 2020.

[16]Ho, S. S., B. P. Hung, N. Heyrani, M. A. Lee, and J. K. Leach. Hypoxic preconditioning of mesenchymal stem cells with subsequent spheroid formation accelerates repair of segmental bone defects. *Stem Cells.* 36(9):1393–1403, 2018.

[17]Hu, W., S. Zhu, M. L. Fanai, J. Wang, J. Cai, and J. Feng. 3D co-culture model of endothelial colony-forming cells (ecfcs) reverses late passage adipose-derived stem cell senescence for wound healing. *Stem Cell Res. Ther.* 11(1):355, 2020.

[18]Huang, Y. Z., M. Gou, L. C. Da, W. Q. Zhang, and H. Q. Xie. Mesenchymal stem cells for chronic wound healing: Current status of preclinical and clinical studies. *Tissue Eng. Part B.* 26(6):555–570, 2020.

[19]Jiao, Z., Y. Ma, Q. Zhang, Y. Wang, T. Liu, X. Liu, et al. The adipose-derived mesenchymal stem cell secretome promotes hepatic regeneration in miniature pigs after liver ischaemia-reperfusion combined with partial resection. *Stem Cell Res. Ther.* 12(1):218, 2021.

[20]Kuss, M. A., S. Wu, Y. Wang, J. B. Untrauer, W. Li, J. Y. Lim, et al. Prevascularization of 3d printed bone scaffolds by bioactive hydrogels and cell co-culture. *J. Biomed. Mater. Res. B.* 106(5):1788–1798, 2018.

[21]Lee, J. H., Y. S. Han, and S. H. Lee. Long-duration three-dimensional spheroid culture promotes angiogenic activities of adipose-derived mesenchymal stem cells. *Biomol. Ther. (Seoul).* 24(3):260–267, 2016.

[22]Liu, S., T. Jiang, R. Guo, C. Li, C. Lu, G. Yang, et al. Injectable and degradable peg hydrogel with antibacterial performance for promoting wound healing. *ACS Appl. Bio Mater.* 4(3):2769–2780, 2021.

[23]Loynes, C. A., J. A. Lee, A. L. Robertson, M. J. Steel, F. Ellett, Y. Feng, et al. Pge2 production at sites of tissue injury promotes an anti-inflammatory neutrophil phenotype and determines the outcome of inflammation resolution in vivo. *Sci. Adv.* 4(9):8320, 2018.

[24]Mead, L. E., D. Prater, M. C. Yoder, and D. A. Ingram. Isolation and characterization of endothelial progenitor cells from human blood. *Curr. Protoc. Stem Cell Biol.* 1:5, 2008.

[25]Murphy, K. C., J. Whitehead, P. C. Falahee, D. Zhou, S. I. Simon, and J. K. Leach. Multifactorial experimental design to optimize the anti-inflammatory and proangiogenic potential of mesenchymal stem cell spheroids. *Stem Cells.* 35(6):1493–1504, 2017.

[26]Phelps, E. A., D. M. Headen, W. R. Taylor, P. M. Thule, and A. J. Garcia. Vasculogenic bio-synthetic hydrogel for enhancement of pancreatic islet engraftment and function in type 1 diabetes. *Biomaterials.* 34(19):4602–4611, 2013.

[27]Rakita, A., N. Nikolic, M. Mildner, J. Matiasek, and A. Elbe-Burger. Re-epithelialization and immune cell behaviour in an ex vivo human skin model. *Sci. Rep.* 10(1):1, 2020.

[28]Rao, R. R., A. W. Peterson, J. Ceccarelli, A. J. Putnam, and J. P. Stegemann. Matrix composition regulates three-dimensional network formation by endothelial cells and mesenchymal stem cells in collagen/fibrin materials. *Angiogenesis.* 15(2):253–264, 2012.

[29]Seebach, C., D. Henrich, C. Kahling, K. Wilhelm, A. E. Tami, M. Alini, et al. Endothelial progenitor cells and mesenchymal stem cells seeded onto beta-tcp granules enhance early vascularization and bone healing in a critical-sized bone defect in rats. *Tissue Eng. Part A.* 16(6):1961–1970, 2010.

[30]Sivamani, R. K. Eicosanoids and keratinocytes in wound healing. *Adv Wound Care (New Rochelle).* 3(7):476–481, 2014.

[31]Skiles, M. L., B. Hanna, L. Rucker, A. Tipton, A. Brougham-Cook, E. Jabbarzadeh, et al. Asc spheroid geometry and culture oxygenation differentially impact induction of preangiogenic behaviors in endothelial cells. *Cell Transplant.* 24(11):2323–2335, 2015.

[32]Vorwald, C. E., S. S. Ho, J. Whitehead, and J. K. Leach. High-throughput formation of mesenchymal stem cell spheroids and entrapment in alginate hydrogels. *Methods Mol Biol.* 1758:139–149, 2018.

[33]Vorwald, C. E., S. Joshee, and J. K. Leach. Spatial localization of endothelial cells in heterotypic spheroids influences notch signaling. *J. Mol. Med. (Berl).* 98(3):425–435, 2020.

[34]Vorwald, C. E., K. C. Murphy, and J. K. Leach. Restoring vasculogenic potential of endothelial cells from diabetic patients through spheroid formation. *Cell Mol. Bioeng.* 11(4):267–278, 2018.

[35]Wu, Y., L. Chen, P. G. Scott, and E. E. Tredget. Mesenchymal stem cells enhance wound healing through differentiation and angiogenesis. *Stem Cells.* 25(10):2648–2659, 2007.

[36]Yang, C., B. Han, C. Cao, D. Yang, X. Qu, and X. Wang. An injectable double-network hydrogel for the co-culture of vascular endothelial cells and bone marrow mesenchymal stem cells for simultaneously enhancing vascularization and osteogenesis. *J. Mater. Chem. B.* 6(47):7811–7821, 2018.

[37]Ylostalo, J. H., T. J. Bartosh, K. Coble, and D. J. Prockop. Human mesenchymal stem/stromal cells cultured as spheroids are self-activated to produce prostaglandin e2 that directs stimulated macrophages into an anti-inflammatory phenotype. *Stem Cells.* 30(10):2283–2296, 2012.

[38]Yu, X., Q. Wan, X. Ye, Y. Cheng, J. L. Pathak, and Z. Li. Cellular hypoxia promotes osteogenic differentiation of mesenchymal stem cells and bone defect healing via stat3 signaling. *Cell Mol. Biol. Lett.* 24:64, 2019.

BMES BIOMEDICAL ENGINEERING SOCIETY